

Inhibition of cytohesins by SecinH3 leads to hepatic insulin resistance

Markus Hafner¹, Anton Schmitz¹, Imke Grüne¹, Seergazhi G. Srivatsan¹, Bianca Paul², Waldemar Kolanus², Thomas Quast², Elisabeth Kremmer³, Inga Bauer¹ & Michael Famulok¹

G proteins are an important class of regulatory switches in all living systems. They are activated by guanine nucleotide exchange factors (GEFs), which facilitate the exchange of GDP for GTP^{1,2}. This activity makes GEFs attractive targets for modulating disease-relevant G-protein-controlled signalling networks^{3–5}. GEF inhibitors are therefore of interest as tools for elucidating the function of these proteins and for therapeutic intervention; however, only one small molecule GEF inhibitor, brefeldin A (BFA), is currently available^{6–9}. Here we used an aptamer displacement screen to identify SecinH3, a small molecule antagonist of cytohesins. The cytohesins are a class of BFA-resistant small GEFs for ADP-ribosylation factors (ARFs), which regulate cytoskeletal organization¹⁰, integrin activation¹¹ or integrin signalling¹². The application of SecinH3 in human liver cells showed that insulin-receptor-complex-associated cytohesins are required for insulin signalling. SecinH3-treated mice show increased expression of gluconeogenic genes, reduced expression of glycolytic, fatty acid and ketone body metabolism genes in the liver, reduced liver glycogen stores, and a compensatory increase in plasma insulin. Thus, cytohesin inhibition results in hepatic insulin resistance. Because insulin resistance is among the earliest pathological changes in type 2 diabetes, our results show the potential of chemical biology for dissecting the molecular pathogenesis of this disease.

Cytohesins are multi-domain proteins in which a Sec7 domain bears the GEF activity. Unlike the large (~200 kDa) ARF-GEFs, the small ones (~47 kDa) are insensitive to BFA^{13,14}. The only known small GEF Sec7-domain inhibitor is the RNA aptamer M69, which represses guanine nucleotide exchange *in vitro* and reduces T-cell adhesion¹⁰. Using M69 and the cytohesin-1 Sec7 domain, we established an assay based on fluorescence polarization to identify cytohesin-specific small molecules that displace the aptamer from its target and adopt its inhibitory activity (see Supplementary Fig. 1a). From a diverse library of synthetic chemicals, we identified a series of 1,2,4-triazole derivatives as initial hits and selected the most promising compound, H3 (Fig. 1a, left), for synthesis and further studies (see Supplementary Figs 1, 2). H3 bound to the Sec7 domains of human cytohesins-1–3 with dissociation constants (K_d values) between 200 and 250 nM (Table 1). H3e, H3ip and H3bio, in which substituent R_1 is increased (see Supplementary Fig. 2), showed gradually decreased Sec7 affinity. The Sec7 domain of EFA6, an ARF6-GEF that does not belong to the cytohesin family, was bound about 30-fold more weakly, despite its 32% identity and 46% similarity with the cytohesin-1 Sec7 domain. The CDC25-like domain of the ras-GEF Son of sevenless (Sos) was not bound.

To assess the compound's inhibitory potential, guanine nucleotide exchange assays were performed with ARF1 and full-length

cytohesins^{15,16}. All cytohesins, including the mouse and *Drosophila* homologues of cytohesin-3, exhibited half-maximal inhibitory concentrations (IC₅₀ values) between 2.4 and 5.6 μ M (Table 1), indicating that H3 recognizes an evolutionarily conserved region. For EFA6–Sec7 and Gea2–Sec7, a large GEF from yeast, the IC₅₀s were 18- and 12-fold higher, respectively. The GEF activity of Sos was unaffected. Because of its inhibitory profile, we named the new compound class Secins (for Sec7 inhibitors).

To test whether SecinH3 maintained its *in vitro* preference for cytohesins in living cells, we monitored its effect on the structural integrity of the Golgi apparatus, which depends on the function of BFA-sensitive large GEFs¹⁷. Treatment with 20 μ M BFA completely disrupted Golgi integrity (Fig. 1b, panel 2), whereas treatment with SecinH3 caused a minor effect only at or beyond 50 μ M, consistent with this concentration being close to the IC₅₀ for the large GEF Gea2 (Fig. 1b, panels 3, 4). In summary, these data show that SecinH3 is a Sec7-specific GEF inhibitor with preference for the small GEFs of the cytohesin family.

Four different but highly homologous cytohesins are known in mammals, whereas only one, the cytohesin homologue steppe,

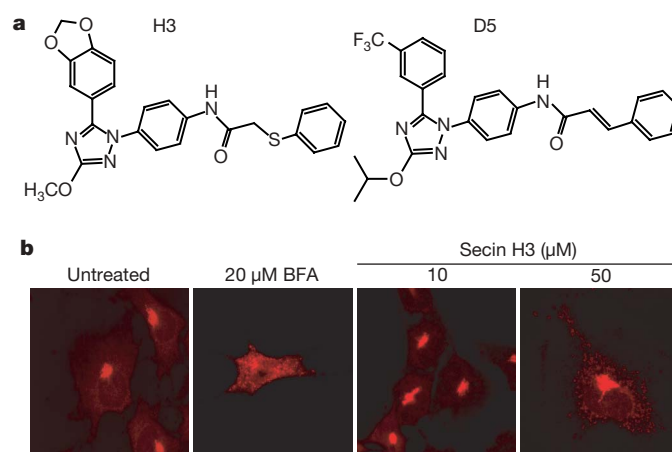


Figure 1 | Structure and characterization of SecinH3. a, Molecular structures of SecinH3 (left) and the negative control compound D5 (right). For details on the synthesis and characterization of each compound, see Supplementary Methods and Supplementary Fig. 2. **b**, SecinH3 does not affect Golgi structure. Compared to untreated cells, no significant disturbance of Golgi integrity is observed at SecinH3 concentrations of 10 μ M and 50 μ M, respectively, whereas BFA leads to complete Golgi destruction at 20 μ M. Golgi membranes were visualized using an anti-galactin antibody.

¹LIMES Program Unit Chemical Biology & Medicinal Chemistry, c/o Kekulé Institut für Organische Chemie und Biochemie, University of Bonn, Gerhard-Domagk-Straße 1, 53121 Bonn, Germany. ²LIMES Program Unit Molecular Immune and Cell Biology, Laboratory of Molecular Immunology, University of Bonn, Karlrobert-Kreiten Straße 13, 53115 Bonn, Germany. ³Institut für Molekulare Immunologie, GSF-Forschungszentrum für Umwelt und Gesundheit, Marchioninistr. 25, 81377 München, Germany.

Table 1 | SecinH3 binds cytohesin Sec7 domains and inhibits GDP/GTP exchange

Protein	Dissociation constant, K_d (nM)*				Inhibition of GDP/GTP exchange, IC_{50} (μ M)†		
	H3	H3e	H3ip	H3bio	Protein	H3	D5
hCyh1-S7	200 ± 10				hCyh1	5.4 ± 0.3	n.d.‡
hCyh2-S7	250 ± 5	305 ± 15	370 ± 18	523 ± 26	hCyh2	2.4 ± 0.1	n.d.‡
hCyh3-S7	239 ± 17				hCyh3	5.6 ± 0.4	
					mCyh3	5.4 ± 0.6	
					steppke§	5.6 ± 0.2	
					yGea2-S7	65 ± 4.0	
hEFA6-S7	7,600 ± 200				hEFA6-S7	>100	
hSos	n.d.‡				hSos	n.d.‡	

* Measured by isothermal titration calorimetry (see Supplementary Fig. 3).

† GTP exchange of the indicated full-length GEFs or GEF-Sec7 domains on ARF1 was measured using the tryptophan fluorescence assay.

‡ n.d., not detectable.

§ *Drosophila* homologue of cytohesins.

|| Sos-catalysed GTP exchange on Ras was measured by the mantGDP assay.

exists in flies. So far, no cytohesin knockout mouse has been described, but flies lacking steppke show reduced growth¹⁸, suggesting that it is involved in insulin signalling. We tested the requirement for mammalian cytohesins in insulin signalling by monitoring the transcription of the prototypic insulin-regulated gene for insulin-like growth factor binding protein 1 (*IGFBP1*) in the human liver cell line HepG2. SecinH3 almost completely blocked the insulin-dependent transcriptional repression of *IGFBP1* (Fig. 2a) with an IC_{50} of 2.2 μ M (see Supplementary Fig. 4; see Supplementary Information and

Nature Protocols doi: 10.1038/nprot.2006.413 for details of methods). D5, a structurally related compound (Fig. 1a, right) that was inactive in the aptamer displacement and GDP/GTP exchange assays (see Supplementary Fig. 1b; Table 1) did not affect insulin-dependent levels of *IGFBP1* mRNA (Fig. 2a). To analyse whether SecinH3 affects ARF activation by cytohesins in living cells we used immobilized GGA3 (Golgi-associated, gamma adaptin ear containing, ARF binding protein 3) to capture activated, GTP-bound ARF¹⁹ (see Supplementary Methods and *Nature Protocols* doi: 10.1038/nprot.2006.412 for detailed methods). Insulin stimulation increased the level of ARF6-GTP that was pulled down with GGA3, which was reduced in SecinH3-treated cells but remained unaffected by D5 (Fig. 2b). Consistently, insulin-stimulated translocation of ARF6 to the plasma membrane was also inhibited by SecinH3 (see Supplementary Fig. 5). Finally, SecinH3 had no direct effect on various kinases, including those involved in insulin signalling (Supplementary Table 1).

To confirm that SecinH3 affects insulin signalling by inhibition of cytohesins, we knocked down cytohesins 1–3 (*cyh1–3*), the only expressed cytohesins in HepG2 cells (data not shown), by RNA interference and analysed gene expression (Fig. 2c). Quantitative PCR (qPCR) and western blotting confirmed the specificity of siRNAs for their respective target mRNAs (see Supplementary Fig. 6). Whereas the knock-down of *cyh1* did not prevent the insulin-dependent repression of *IGFBP1* expression, knockdown of *cyh3* inhibited the insulin effect to a similar level as with SecinH3, and knockdown of *cyh2* had an even stronger effect. An ARF6-specific siRNA also inhibited the insulin effect whereas an ARF1-specific siRNA did not (see Supplementary Fig. 7).

Expression of *IGFBP1* is controlled by insulin acting through the forkhead box transcription factors FoxO1A and FoxO3A. Upon insulin stimulation, protein kinase B (PKB/Akt) is activated by phosphorylation and translocates to the nucleus, where it phosphorylates FoxO proteins^{20,21} leading to their nuclear exclusion and, thus, reduction of target gene expression^{22,23}. We found that SecinH3 inhibited the insulin-dependent phosphorylation of Akt and FoxO1A in a concentration-dependent manner (Fig. 2d; Supplementary Fig. 8). Morphological analysis of HepG2 cells transfected with enhanced green fluorescent protein (EGFP)-tagged FoxO1A showed that the insulin-induced exclusion of FoxO1A from the nucleus was completely prevented by SecinH3 (see Supplementary Fig. 9).

Metabolic insulin signalling in the target cell is initiated by insulin binding to the insulin receptor, which undergoes autophosphorylation on cytoplasmic tyrosine residues. This is followed by binding and phosphorylation of specific tyrosines in the insulin receptor substrate (IRS) proteins. The phosphotyrosines of pIRS serve as binding sites for phosphatidylinositol-3-OH kinase (PI(3)K), which then activates its downstream targets, including Akt²⁴. Neither autophosphorylation of the insulin receptor nor its density on the HepG2 cell surface was affected by SecinH3 (see Supplementary Fig. 10), showing that cytohesins act after receptor activation. However, the next step, activation of IRS1 by its phosphorylation, was inhibited

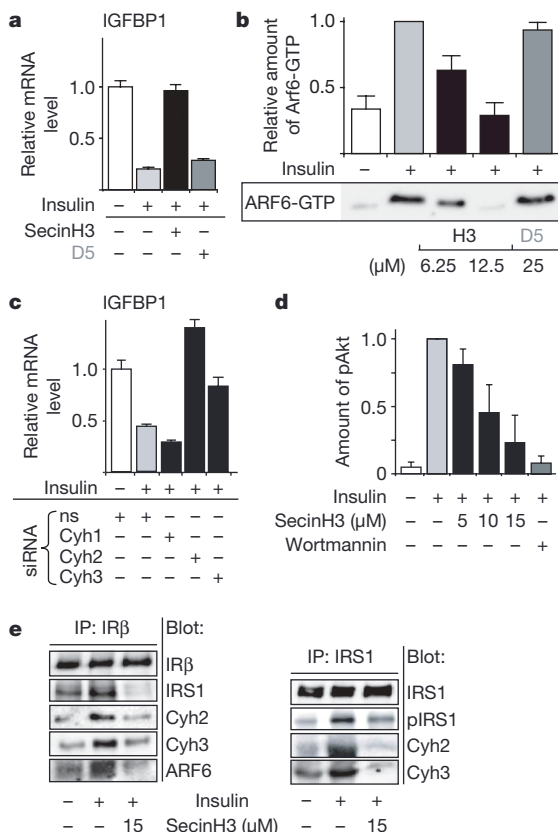


Figure 2 | SecinH3 inhibits insulin signalling in HepG2 cells. a, Effect of SecinH3 on insulin-dependent *IGFBP1* expression, determined by quantitative PCR (qPCR) ($n = 3$). **b**, Insulin-induced ARF activation is inhibited by SecinH3 ($n = 4$). Lower panel: representative western blot of activated ARF6. **c**, Cells were transfected with the indicated siRNA or non-silencing control siRNA (ns) and *IGFBP1* expression was determined by qPCR ($n = 3$). **d**, SecinH3 reduces Akt phosphorylation. pAkt was detected by immunoblot (see Supplementary Fig. 8), using actin for normalization ($n > 6$). **e**, Effect of SecinH3 on insulin receptor and IRS1 complex formation. IR β (left) and IRS1 (right) were immunoprecipitated, and coprecipitated proteins were detected by immunoblotting. Error bars: s.d.

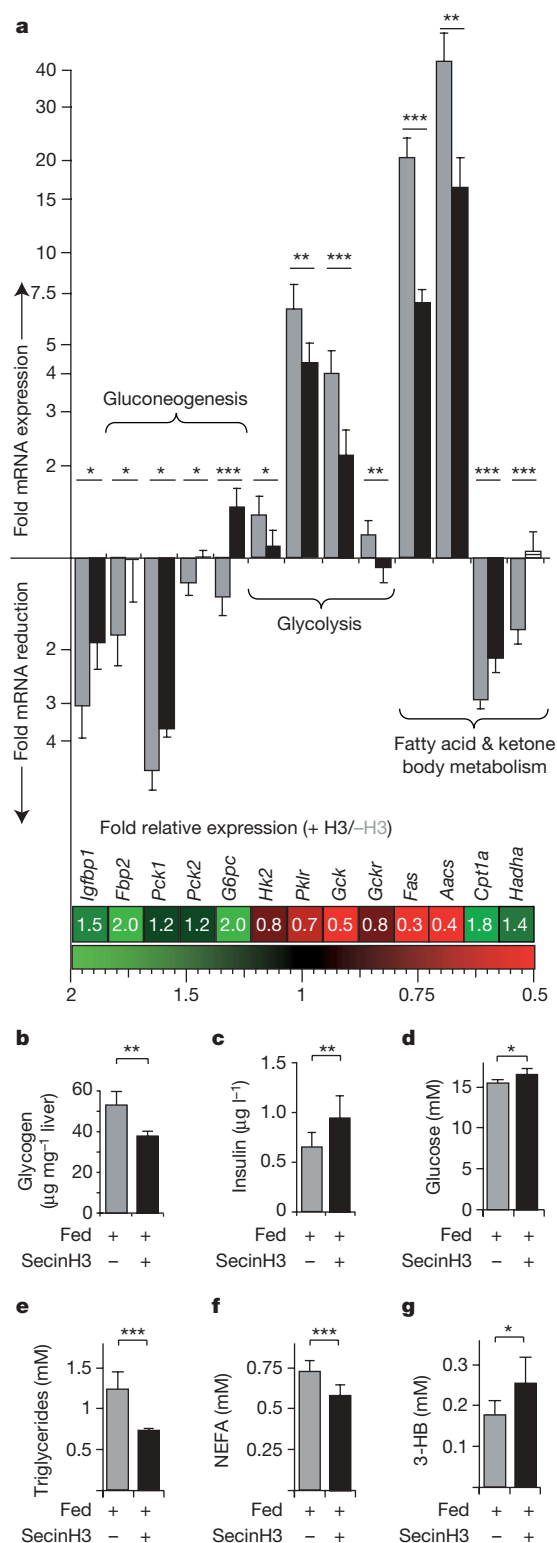


Figure 3 | Impaired cytohesin function results in hepatic insulin resistance.

a, Gene expression in liver was determined by qPCR in mice fed with (black) or without SecinH3 (grey). Upper part: change in gene expression as compared to starved animals (set as 1). Lower part: ratio of gene expression in SecinH3-fed versus control animals ($n = 6$). Insulin-repressed genes are overexpressed (green); insulin-induced genes are underexpressed (red).

b, Glycogen levels³¹ in livers of SecinH3-fed and control mice, expressed as μg glucose units per mg liver ($n = 5$). Serum levels of insulin (**c**), glucose (**d**), triglycerides (**e**), non-esterified fatty acids (NEFA) (**f**) and 3-hydroxybutyrate (3-HB) (**g**) were determined in non-starved SecinH3-fed and control mice ($n = 8$). * $P < 0.05$, ** $P < 0.01$, *** $P < 0.001$. Error bars: s.d.

by SecinH3 (see Supplementary Fig. 11). Co-immunoprecipitation studies revealed insulin-dependent interactions of *cyh2*, *cyh3*, and ARF6 with the insulin receptor–IRS1 complex, which were reduced in the presence of SecinH3 (Fig. 2e). The binding of IRS1 to the insulin receptor was also inhibited by SecinH3, indicating that the cytohesin–ARF6 complex facilitates the formation of the insulin receptor–IRS1 complex. These results show that *cyh2* and *cyh3* are fundamentally involved in the earliest steps of insulin signalling. We propose that the insulin-dependent physical association of the cytohesin–ARF6 complex with the insulin receptor–IRS complex is required for the phosphorylation of IRS and thus for the activation of the insulin signalling cascade immediately at the insulin receptor.

We next investigated the involvement of cytohesins in insulin signalling *in vivo*, by feeding mice chow containing SecinH3. Liquid chromatography–mass spectrometry analysis verified that livers from SecinH3-fed mice contained the unaltered compound (see Supplementary Fig. 12; method is described in detail in Supplementary Information and *Nature Protocols* doi: 10.1038/nprot.2006.414). Besides *Igfbp1*, we analysed hepatic expression of the genes for pyruvate carboxykinase-1 and -2 (*Pck1*, *Pck2*), fructose-1,6-bisphosphatase 2 (*Fbp2*) and glucose-6-phosphatase (*G6pc*), which are involved in gluconeogenesis, and the glycolytic enzymes glucokinase (*Gck*), its regulator (*Gckr*), pyruvate kinase (*Pklr*), and hexokinase 2 (*Hk2*). Compared to mice fed the same chow without SecinH3, the expression levels of the insulin-repressed gluconeogenic genes were elevated (green in Fig. 3a), whereas the insulin-induced glycolytic genes were reduced (red in Fig. 3a). Insulin-stimulated Akt phosphorylation was also inhibited in SecinH3-treated mice (see Supplementary Fig. 13). Analysis of liver glycogen levels revealed that the compound also inhibited insulin-dependent glycogen synthesis (Fig. 3b). SecinH3 also inhibited the insulin-induced expression of the genes for fatty acid synthase (*Fasn*) and acetoacetyl-CoA synthetase (*Aacs*), which are involved in triglyceride synthesis and ketone body metabolism, respectively (Fig. 3a). The expression of the genes for two key enzymes of mitochondrial β -oxidation, carnitine palmitoyltransferase 1a (*Cpt1a*) and hydroxyacyl-CoA dehydrogenase (*Hadha*), both of which are repressed by insulin, was increased in the SecinH3-treated mice (Fig. 3a).

All available biochemical and gene expression data therefore converge on the view that cytohesins are fundamentally involved in insulin signalling and that their impairment results in physiological alterations that are characteristic of hepatic insulin resistance. Insulin resistance is an important hallmark of the pre-clinical stages of type 2 diabetes; organisms compensate for this by increasing insulin secretion to maintain blood glucose at physiological levels. We found significantly increased levels of serum insulin with slightly elevated glucose concentrations in SecinH3-treated mice (Fig. 3c, d). In accordance with the reduced *Fas* expression, serum triglycerides (Fig. 3e) and non-esterified fatty acids (Fig. 3f) were reduced. Enhanced β -oxidation due to elevated *Cpt1a* and *Hadha* levels, which leads to increased generation of acetyl-CoA together with reduced acetoacetate consumption by *Aacs*, should raise the levels of ketone bodies. Accordingly, 3-hydroxybutyrate was increased in the serum of SecinH3-treated mice (Fig. 3g). In summary, the effects of the cytohesin inhibitor SecinH3 on insulin signalling and gene expression in the liver, and the resulting physiological alterations, correspond to the pathological changes seen in mice with a liver-specific insulin receptor knockout²⁵ (see Supplementary Table 2), indicating that not only are cytohesins required for insulin signalling in the liver, but their dysfunction also contributes to the pathogenesis of hepatic insulin resistance.

Insulin resistance is considered to have a causative role in the pathogenesis of type 2 diabetes²⁶. However, the molecular mechanism that leads to impaired insulin sensitivity is poorly understood. Knockout of either the insulin receptor²⁵ or IRS-2 (refs 27, 28), or the liver-specific expression of a constitutively active form of FoxO1 (ref. 29) in transgenic mice, results in hepatic insulin resistance.

Because mutations of these genes have not been described for most patients suffering from type 2 diabetes³⁰, additional factors seem to be involved. Our data indicate that cytohesins might be one of these factors and that their function might be crucial for regulating the sensitivity of insulin-responsive tissues.

Furthermore, we show here how to translate information stored within an aptamer into a small molecule. Thereby, chemical space can be explored in a rapid, focused, and modular manner, by indirectly taking advantage of the highest molecular diversity currently amenable to screening, namely that of up to 10^{16} different nucleic acid sequences. Aptamer displacement screens demand small molecules of high initial potency, leading to effective and specific inhibitors that can be used as drug leads or tools in chemical biology.

METHODS

Details of aptamer labelling and the aptamer displacement screen, determination of $K_{d,s}$ by isothermal titration calorimetry, GDP/GTP exchange assays, the ARF6 activation assay, mice, quantification of *Igfbp1* expression in cell culture, quantification of gene expression in mouse liver, siRNA transfections, immunoblotting and immunoprecipitation, determination of physiological parameters, synthesis and characterization of compounds, and the characterization of the cytohesin-3 antibody are provided in Supplementary Information.

Statistics. Results are given as the mean \pm s.d. Statistical analyses were performed by the two-tailed *t*-test using the InStat program (GraphPad). All data sets passed the Kolmogorov and Smirnov test for gaussian distribution. Where the standard deviations of the compared pairs were different, the Welch correction was applied to the *t*-test. Differences of means were considered significant at a significance level of 0.05.

Received 21 September; accepted 3 November 2006.

- Cherfils, J. & Chardin, P. GEFs: structural basis for their activation of small GTP-binding proteins. *Trends Biochem. Sci.* **24**, 306–311 (1999).
- Jackson, C. L. & Casanova, J. E. Turning on ARF: the Sec7 family of guanine-nucleotide-exchange factors. *Trends Cell Biol.* **10**, 60–67 (2000).
- Hashimoto, S. *et al.* Requirement for Arf6 in breast cancer invasive activities. *Proc. Natl Acad. Sci. USA* **101**, 6647–6652 (2004).
- Gonzalez-Garcia, A. *et al.* RalGDS is required for tumor formation in a model of skin carcinogenesis. *Cancer Cell* **7**, 219–226 (2005).
- Malliri, A. *et al.* Mice deficient in the Rac activator Tiam1 are resistant to Ras-induced skin tumours. *Nature* **417**, 867–871 (2002).
- Donaldson, J. G., Finazzi, D. & Klausner, R. D. Brefeldin A inhibits Golgi membrane-catalysed exchange of guanine nucleotide onto ARF protein. *Nature* **360**, 350–352 (1992).
- Helms, J. B. & Rothman, J. E. Inhibition by brefeldin A of a Golgi membrane enzyme that catalyses exchange of guanine nucleotide bound to ARF. *Nature* **360**, 352–354 (1992).
- Morinaga, N., Tsai, S.-C., Moss, J. & Vaughan, M. Isolation of a brefeldin A-inhibited guanine nucleotide-exchange protein for ADP ribosylation factor (ARF) 1 and ARF3 that contains a Sec7-like domain. *Proc. Natl Acad. Sci. USA* **93**, 12856–12860 (1996).
- Peyroche, A. *et al.* Brefeldin A acts to stabilize an abortive ARF–GDP–Sec7 domain protein complex: involvement of specific residues of the Sec7 domain. *Mol. Cell Biol.* **3**, 275–285 (1999).
- Mayer, G. *et al.* Controlling small guanine-nucleotide-exchange factor function through cytoplasmic RNA intramers. *Proc. Natl Acad. Sci. USA* **98**, 4961–4965 (2001).
- Kolanus, W. *et al.* $\alpha\beta 2$ integrin/LFA-1 binding to ICAM-1 induced by cytohesin-1, a cytoplasmic regulatory molecule. *Cell* **86**, 233–242 (1996).
- Perez, O. D. *et al.* Leukocyte functional antigen 1 lowers T cell activation thresholds and signaling through cytohesin-1 and Jun-activating binding protein 1. *Nature Immunol.* **4**, 1083–1092 (2003).
- Renault, L., Guibert, B. & Cherfils, J. Structural snapshots of the mechanism and inhibition of a guanine nucleotide exchange factor. *Nature* **426**, 525–530 (2003).

- Mossessova, E., Corpina, R. A. & Goldberg, J. Crystal structure of ARF1*Sec7 complexed with Brefeldin A and its implications for the guanine nucleotide exchange mechanism. *Mol. Cell* **12**, 1403–1411 (2003).
- Kruljac-Leticic, A., Moelleken, J., Kallin, A., Wieland, F. & Blaukat, A. The tyrosine kinase Pyk2 regulates Arf1 activity by phosphorylation and inhibition of the Arf-GTPase-activating protein ASAP1. *J. Biol. Chem.* **278**, 29560–29570 (2003).
- Ahmadian, M. R., Wittinghofer, A. & Herrmann, C. Fluorescence methods in the study of small GTP-binding proteins. *Methods Mol. Biol.* **189**, 45–63 (2002).
- Moss, J. & Vaughan, M. Molecules in the ARF Orbit. *J. Biol. Chem.* **273**, 21431–21434 (1998).
- Fuss, B., Becker, T., Zinke, I. & Hoch, M. The cytohesin Steppke is essential for insulin signalling in *Drosophila*. *Nature* doi:10.1038/nature05412 (this issue).
- Takatsu, H., Yoshino, K., Toda, K. & Nakayama, K. GGA proteins associate with Golgi membranes through interaction between their GGAH domains and ADP-ribosylation factors. *Biochem. J.* **365**, 369–378 (2002).
- Brunet, A. *et al.* Akt promotes cell survival by phosphorylating and inhibiting a Forkhead transcription factor. *Cell* **96**, 857–868 (1999).
- Kops, G. J. *et al.* Direct control of the Forkhead transcription factor AFX by protein kinase B. *Nature* **398**, 630–634 (1999).
- Burgering, B. M. & Kops, G. J. Cell cycle and death control: long live Forkheads. *Trends Biochem. Sci.* **27**, 352–360 (2002).
- Accili, D. & Arden, K. C. FoxOs at the crossroads of cellular metabolism, differentiation, and transformation. *Cell* **117**, 421–426 (2004).
- Knight, Z. A. *et al.* A pharmacological map of the PI3-K family defines a role for p110 α in insulin signaling. *Cell* **125**, 733–747 (2006).
- Michael, M. D. *et al.* Loss of insulin signaling in hepatocytes leads to severe insulin resistance and progressive hepatic dysfunction. *Mol. Cell* **6**, 87–97 (2000).
- Biddinger, S. B. & Kahn, C. R. From mice to men: insights into the insulin resistance syndromes. *Annu. Rev. Physiol.* **68**, 123–158 (2006).
- Kubota, N. *et al.* Disruption of insulin receptor substrate 2 causes type 2 diabetes because of liver insulin resistance and lack of compensatory beta-cell hyperplasia. *Diabetes* **49**, 1880–1889 (2000).
- Withers, D. J. *et al.* Disruption of IRS-2 causes type 2 diabetes in mice. *Nature* **391**, 900–904 (1998).
- Nakae, J. *et al.* Regulation of insulin action and pancreatic beta-cell function by mutated alleles of the gene encoding forkhead transcription factor Foxo1. *Nature Genet.* **32**, 245–253 (2002).
- Malecki, M. T. S. Genetics of type 2 diabetes mellitus. *Diabetes Res. Clin. Pract.* **68**, S10–S21 (2005).
- Mora, A., Lipina, C., Tronche, F., Sutherland, C. & Alessi, D. R. Deficiency of PDK1 in liver results in glucose intolerance, impairment of insulin-regulated gene expression and liver failure. *Biochem. J.* **385**, 639–648 (2005).

Supplementary Information is linked to the online version of the paper at www.nature.com/nature.

Acknowledgements We thank M. Franco for ARF6 and EFA6 plasmids, R. Quirion for the EGFP–FoxO1A plasmid, J. Kuriyan for the Ras and Sos plasmids, J.-L. Parent for the GST–GGA3 plasmid, M. Hoch for the steppke plasmid, V. Fieberg, K. Rotscheldt, N. Kuhn, R. Tolba, and A. Carney for technical assistance and the members of the Famulok laboratory for helpful discussions. This work was supported by grants from the Deutsche Forschungsgemeinschaft, the Sonderforschungsbereiche 645 and 704, the Fonds der Chemischen Industrie (to M.F.), and the Alexander von Humboldt foundation (to S.G.S.).

Author Contributions M. H. and A.S. contributed equally to this work. M.H. and A.S. performed and designed, with M.F., most of the included studies. I.G. performed the aptamer displacement screen and binding and *in vitro* inhibition analyses of Secins. S.G.S. synthesized all Secin derivatives. W.K. provided cytohesin and ARF expression plasmids, E.K. produced the cyh3 monoclonal antibody and B.P. characterized it. T.Q. performed the analysis of Golgi integrity and ARF6 membrane recruitment. I.B. and A.S. did the immunoprecipitation experiments. M.F. supervised the research project, and assisted in the experimental design. All authors discussed the experimental results. A.S. and M.F. wrote the manuscript.

Author Information Reprints and permissions information is available at www.nature.com/reprints. The authors declare no competing financial interests. Correspondence and requests for materials should be addressed to M.F. (m.famulok@uni-bonn.de).